



## Tempol attenuates chronic intermittent hypoxia-induced lung injury through the miR-145-5p/Nrf2 signaling pathway

Li Ai, Yongxia Li\*, Zhijuan Liu, Ran Li, Xiaona Wang, Bing Hai

Department of Respiratory and Critical Care Medicine, The Second Affiliated Hospital of Kunming Medical University, Kunming 650101, Yunnan, China

### ARTICLE INFO

#### Original paper

#### Article history:

Received: June 25, 2023

Accepted: November 13, 2023

Published: December 10, 2023

#### Keywords:

Tempol, miR-145-5p/Nrf2, obstructive sleep apnea, lung injury, oxidative stress

### ABSTRACT

This study mainly explored the effect of Tempol on OSA-induced lung injury and the specific molecular mechanism. A hypoxia/reoxygenation (H/R) cell model and an IH-induced lung injury model in rats were constructed. The expression of related genes and proteins was detected by RT-qPCR and Western blotting. HE and Masson staining were used to observe the pathological changes in lung tissues. The expression levels of inflammatory cytokines were detected by ELISA. Apoptotic cells were observed by TUNEL. The ROS levels were detected by a DCFH-DA probe. Tempol administration effectively reduced the pathological changes in lung tissue and the progression of pulmonary fibrosis in rats with lung injury and reduced the expression of inflammatory factors. miR-145-5p was significantly upregulated in rats with IH-induced lung injury, and Tempol treatment inhibited the expression of miR-145-5p. Transfection with the miR-145-5p inhibitor effectively inhibited H/R cell apoptosis and autophagy, while transfection with the miR-145-5p mimic had the opposite effect. Targeting miR-145-5p negatively regulates the expression of Nrf2. Transfection of the miR-145-5p mimic weakened the inhibitory effects of Tempol on apoptosis and autophagy in H/R cells. Overexpression of the Nrf2 reversed the effects of the miR-145-5p mimic on Tempol to a certain extent. It was also confirmed in animal experiments that overexpression of Nrf2 reversed the inhibitory effect of the miR-145-5p mimic on Tempol's lung injury relief effect. Tempol alleviates lung injury induced by chronic intermittent hypoxia by regulating the miR-145-5p/Nrf2 molecular axis and inhibiting autophagy.

Doi: <http://dx.doi.org/10.14715/cmb/2023.69.13.34>

Copyright: © 2023 by the C.M.B. Association. All rights reserved.

### Introduction

Obstructive sleep apnea (OSA) is a frequently diagnosed sleep-breathing disease that affects millions of people around the world to varying degrees and is closely associated with the occurrence of more diseases or increased risk of major causes of death (1). OSA is a respiratory distress disorder characterized by snoring sleep architecture disorders, frequent oxygen desaturation and daytime sleepiness (2). Then, chronic intermittent hypoxia (CIH) causes oxidative stress and inflammatory responses (3). Yanyan Hou et al. (4) confirmed that CIH caused epithelial-mesenchymal transition (EMT), accelerated the deposition of lung collagen, and finally led to lung tissue injury. For many patients with lung disease, available evidence suggests that prompt identification and treatment of sleep-disordered breathing can improve their quality of life and may alter their course. Therefore, searching for molecular mechanisms that can effectively improve OSA and regulate oxidative stress may become a new approach to the treatment of OSA.

Nuclear factor-erythroid 2-related factor 2 (Nrf2) is a transcription factor capable of antioxidation and inflammation that maintains the endogenous redox balance within cells, as well as controls cellular metabolism, cytoprotection, immunity and tumorigenesis (5). Under physiological conditions, Nrf2 functions by binding to its negative regulators, and the binding of Nrf2 to its endogenous inhi-

tor Keap1 is ubiquitous in cells (6). Nrf2/Keap1 localizes in the cytoplasm and targets proteasome degradation under basal conditions, promoting intracellular defense mechanisms to counteract oxidative stress and regulate inflammation (7). Many studies have proven that Nrf2 regulates the expression of antioxidant and anti-inflammatory genes in the lung, which is a key regulatory factor of lung injury. For example, Jia Yan et al. (8) reported that Nrf2 prevents acute lung injury (ALI) and inflammation by regulating TLR4/Akt signaling. Weixiang Xu et al. (9) found that the Nrf2/NF- $\kappa$ B pathway played a protective role in lung oxidative damage and inflammation induced by ochratoxin. Liming Jia et al. (5) also found that upregulation of the Nrf2/HO-1 signaling pathway could reduce hyperoxygen-induced ALI in mice. Therefore, Nrf2 was chosen as an important entry point for this study.

The superoxide dismutase analog Tempol is a cyclic nitrogen oxide that easily penetrates biological systems (10). The compound is rapidly and reversibly translocated between the three forms of nitrate, hydroxylamine, and oxyammonium cations, eliminates a variety of oxidatively active substances in cells, reduces tissue levels of superoxide ( $O_2^-$ ) and hydrogen peroxide ( $H_2O_2$ ), and reduces oxidative processes. Thus, Tempol protects cells and tissues from oxidative damage. Woo Hyun Park's study confirmed the above in lung cancer cells (11). In addition, another study found that Tempol prevented oxidative stress in the lungs of mice by upregulating some Nrf2-re-

\* Corresponding author. Email: [liyongxia0720@126.com](mailto:liyongxia0720@126.com)

lated genes (12). Therefore, due to the unique regulatory mechanism of Tempol, it was selected as the focus of this study.

MicroRNAs are a class of powerful small RNAs that have been discovered and studied in recent years; they can silence or degrade mRNA and then metabolize and degrade mRNA in biological processes and regulation of death (13). Some studies have found that there are associations between genes involved in the oxidative stress response and miRNAs. For example, Maria Pelullo et al. (14) found that miR-125b/Nrf2/HO-1 synergistically protected lung airway cells from oxidative stress damage, inflammation and cell apoptosis. Yan Huang et al. (15) reported that miR-27b/Nrf2/HO-1/NF- $\kappa$ B could play a protective role in LPS-induced acute lung injury in mice. In addition, miR-145-5p was found to ameliorate acute lung injury (16,17). We predicted that there was a targeted binding site between miR-145-5p and Nrf2 through bioinformatics software. In addition, it has been reported that dioscin regulates the expression of Nrf2 by regulating miR-145-5p (18). Whether miR-145-5p can also affect the process of IH-induced lung injury by mediating the expression of Nrf2 remains to be further explored.

Based on the above studies, we speculate that Tempol may regulate miR-145-5p to activate the Nrf2, reduce the level of intracellular oxidative stress and the release of inflammatory cytokines, inhibit ROS-mediated apoptosis and autophagy, and thus alleviate chronic intermittent hypoxia-induced lung injury.

## Materials and Methods

### Cell culture and construction of the hypoxia/reoxygenation (H/R) model

The lung epithelial cell line BEAS-2B (Otwo Biotech, Shenzhen, China) was selected for experiments and was grown and passaged in Dulbecco's Modified Eagle Medium (DMEM, meilunbio, Dalian, China) containing 10% fetal bovine serum and 1% streptomycin in 5% CO<sub>2</sub> at 37°C. The cell morphology was observed by microscopy, and the culture medium was changed and passaged routinely. Cells were placed in a semipermeable membrane (Lumox ®; Sarstedt, Nuernbrecht, Germany) for rapid gas exchange. Hypoxia/reoxygenation (H/R) cell models were constructed. Cells were hypoxic (37°C, 0% O<sub>2</sub> and 5% CO<sub>2</sub>), incubated with DPBS, reoxygenated and incubated with DMEM culture for 20 h.

### Construction of an IH-induced lung injury model in rats

Male Wistar rats (produced by HFK Bioscience Co, LTD, Beijing, China) were fed normally. The rats were randomly divided into 7 groups (n=12 rats/group). Normal oxygen control group (NC): the flow rate of circulating injected air in the cabin was 3 L/min in 30 s and 3 L/min

in 90 s, and the oxygen concentration was maintained at 21%. Chronic intermittent hypoxia group (IH): circulate nitrogen in the oxygen chamber for 30 s, flow rate of 10 L/min, air for 40 s, flow rate of 10 L/min (reoxygenation time), air flow rate of 5 L/min (normal oxygen maintenance time) for 50 s, and every 2 minutes was 1 cycle so that the oxygen concentration in the chamber could circulate between 5% and 21%. NC+Tempol group: 10% Tempol was injected intraperitoneally 30 minutes before entering the normal oxygen chamber and was subsequently treated as the NC group. IH+Tempol group: 10% Tempol was injected intraperitoneally 30 minutes before entering the hypoxic chamber. IH+NC mimic+Tempol group: 10% Tempol was injected intraperitoneally 30 minutes before entering the hypoxic chamber, and NC mimic was injected into the tail vein. IH+miR-145a-5p mimic+Tempol group: 10% Tempol was injected intraperitoneally 30 minutes before entering the hypoxic chamber, and miR-145a-5p mimic was injected into the tail vein. IH+miR-145a-5p mimic+OE-Nrf2+Tempol group: 10% Tempol was injected intraperitoneally 30 minutes before entering the hypoxic chamber, and miR-145a-5p mimic+OE-Nrf2 was injected into the tail vein. Groups 3-7 were subsequently treated as the IH group. The test time is 9 AM to 5 PM every day. After 8 weeks of continuous treatment, the rats were euthanized, and blood samples and lung tissues were collected for subsequent experiments.

### Determination of ROS levels by the DCFH-DA probe

ROS was determined using the reactive oxygen (ROS) fluorescence probe (D6470, Solarbio, Beijing, China), a DCFH-DA immunofluorescence probe, according to the manufacturer's instructions. BEAS-2B cells were removed from the medium, stained with DCFH-DA and incubated at 37°C for 30 min. The dye was removed with preheated Hank's balanced salt solution (HBSS). Then, the green fluorescence in the cells was observed by fluorescence microscopy (BX63, Olympus, Tokyo, Japan).

### RT-qPCR

A TRIzol RNA extraction kit (Invitrogen, Carlsbad, CA, USA) was used to extract total RNA from the collected cells and tissues. RNA (10  $\mu$ g) was reverse-transcribed into cDNA using a reverse transcription kit (TaKaRa, Tokyo, Japan). Then, the cDNA obtained was used as a template for qPCR amplification (50°C for 2 min  $\rightarrow$  95°C for 2 min  $\rightarrow$  95°C for 15 s  $\rightarrow$  60°C for 32 s)  $\times$  40, and U6 was used as the internal reference. Then, the expression levels of genes were calculated using the 2 <sup>$-\Delta\Delta CT$</sup>  method. The primer sequences of miR-145-5p F/miR-145-5p R and U6 F/U6 R are displayed in Table 1.

### Western Blot

Total proteins were extracted from tissues and cells using RIPA buffer (Beyotime, Shanghai, China), and the

Table 1. Primer Sequences.

Genes	Sequences
miR-145-5p	Forward: 5'-GUCCAGUUUCCAGGAAUCCCU-3' Reverse: 5'-GGAUCCUGGGAAAACUGGACUU-3'
U6	Forward: 5'-CTCGCTTCGGCAGCACA-3' Reverse: 5'-AACGCTTCACGAATTTGCGT-3'

protein concentration was determined using a BCA protein detection kit (PC0020, Beijing Sola Biotechnology Co., Ltd., Beijing, China). The protein was isolated by 10% SDS-PAGE and transferred to PVDF membranes by the electrotransfer method. The protein was incubated with 5% skim milk powder for 1 h. Diluted primary antibodies (cleaved-caspase-3, 1:2000; Bax, 1:2000 and Bcl-2, 1:1000) were incubated at 4°C overnight, and an HRP-labeled secondary antibody was incubated at room temperature for 1 h. The membranes were washed and finally assessed for protein expression by an enhanced chemiluminescence (ECL) kit (US EVERBRIGHT INC.) chromogenic.

### HE staining

Rat lung tissues were fixed with 4% paraformaldehyde. After paraffin embedding, 5µm sections were prepared and stained according to the instructions for hematoxylin and eosin staining kits (Cat. No. G1120, Solarbio, Beijing, China). Finally, the pathological changes were examined under a light microscope.

### Masson staining

Masson staining was used to evaluate collagen deposition in rat lung tissues. Collagen appears blue after staining, indicating the degree of pulmonary fibrosis. Rat lung paraffin sections were stained with Masson's Trichrome Stain Kit (Cat. No. G1340, Solarbio, Beijing, China) and dyed with the prepared dyeing solution for 5 min. After rinsing the staining solution, the sections were differentiated with acid ethanol differentiation solution for 15 seconds. After rinsing with distilled water, the sections were blued with Masson bluing solution for 3 min and then washed with distilled water. The staining solution mixed with Lichun red and acid fuchsin was used to stain the specimen, and then, the sections were cleaned with the prepared weak acid working solution and then with 1% phosphomolybdic acid working solution. The cleaned slices were soaked in aniline blue dyeing solution, cleaned with a weak acid working solution, dehydrated with ethanol, and then cleared with xylene. Finally, specimen sections were sealed with neutral gum and photographed under a microscope.

### ELISA

The TNF-α ELISA kit (Solarbio, Beijing, China), IL-6 ELISA kit (Solarbio, Beijing, China) and IL-1β ELISA kit (Solarbio, Beijing, China) were used to detect the expression of TNF-α, IL-6 and IL-1β in cells and rat serum. The serum or cells were centrifuged at 4°C, and the supernatant was used as the sample for detection. Then, the standard was added to the standard well of the enzyme plate, and 100 µL of the sample was added to the sample well. After plate sealing, the plate was oscillated and incubated at room temperature for 120 min. After the liquid was discarded, the plate was washed with lotion, and the antibody was detected by biotinylation and incubated at room temperature for 120 min. After washing the plate, biotin was added to detect the antibody. Enzyme binding was added after washing the plate again. The substrate was added for color development at room temperature and protected from light for 10-20 min before adding the stop solution. Finally, the OD value was detected by a dual-wavelength enzyme-labeling instrument.

### TUNEL detection

After xylene dewaxing and ethanol hydration, rat lung sections were incubated with 100µL protease K working solution at 37°C for 30 min. After washing with PBS three times, 50µL TdT enzymatic reaction solution was incubated at 37 °C for 60 min away from light. After washing with PBS three times, the sections were incubated with 50µL Streptavidin-TRITC solution at 37 °C for 30 min away from light. Then, after washing with PBS three times, the cell nucleus was re-stained with DAPI staining solution, and the reaction was kept away from light at room temperature for 15 min. Then, fluorescence microscopy was used to observe the apoptotic cells.

### Double luciferase reporter gene assay

A sequence containing the Nrf2 3'UTR wild-type (WT) or mutant (MUT) fragment and the binding site of miR-145-5p was inserted into the pmirGLO luciferase target expression vector (PuFei Biology, Shanghai, China) to construct the pmirGLO-Nrf2-WT/MUT luciferase reporter vector. Nrf2-WT or Nrf2-MUT was co-transfected with the miR-145-5p mimic or NC mimic into 293T cells. After transfection for 48 h, the luciferase activity was detected by a dual luciferase reporter test kit (PuFei Biology, Shanghai, China).

### Statistical analysis

Prism 7.0 software (GraphPad) (La Jolla, CA, USA) was used to analyze the data. Data are given as the mean ± standard deviation (SD). For the normal distribution, differences between the two groups were determined by Student's t-test, and comparisons between groups were determined by one-way analysis of variance (ANOVA). P<0.05 was considered statistically significant.

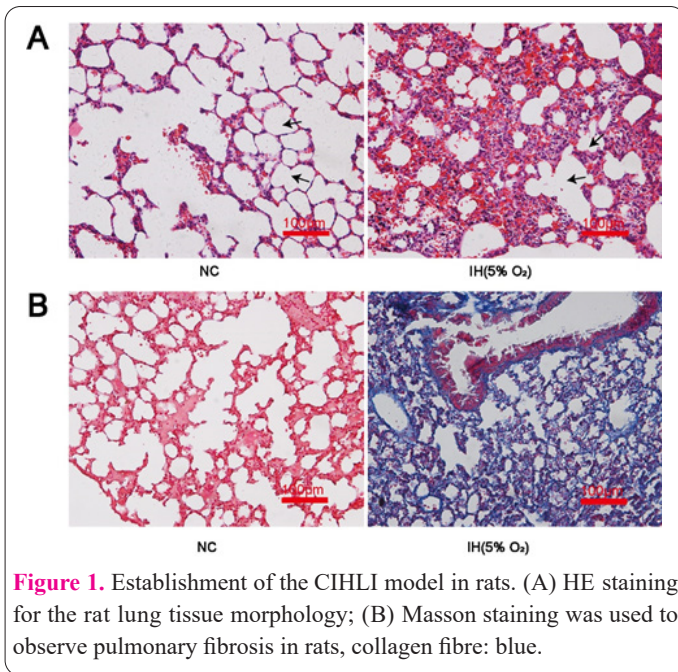
### Results

#### Establishment of the CIHLI model in rats

Lung tissue from Wistar rats treated with normal oxygen treatment and chronic intermittent hypoxia was taken for observation. First, HE staining was used to observe the pathological changes in the lung tissue. The results showed that no obvious pathological damage was observed in the NC group, and there was edema and thickening of the alveolar wall, alveolar fusion, and inflammatory cell infiltration in the lung tissue in the IH group (Figure 1A). Second, Masson staining was used to observe the occurrence of pulmonary fibrosis. The results showed that there was almost no cyanosis (cyanosis was collagen fiber) in the alveolar septa in the NC group, while the normal structure of the alveoli in the IH group was destroyed, fiber foci could be seen, and a large area of cyanosis collagen deposition (blue) was observed (Figure 1B). It is known from the experimental data that the model of CIHLI was successfully established, and follow-up experiments were carried out.

#### Tempol alleviates CIHLI

The lung injury model of Wistar rats was treated with a certain dose of Tempol, and the histological morphology was observed by HE staining. Pathological changes, such as alveolar lysis and lung tissue inflammation, were significantly relieved after Tempol treatment (Figure 2A). Histomorphology was observed by Masson staining, and

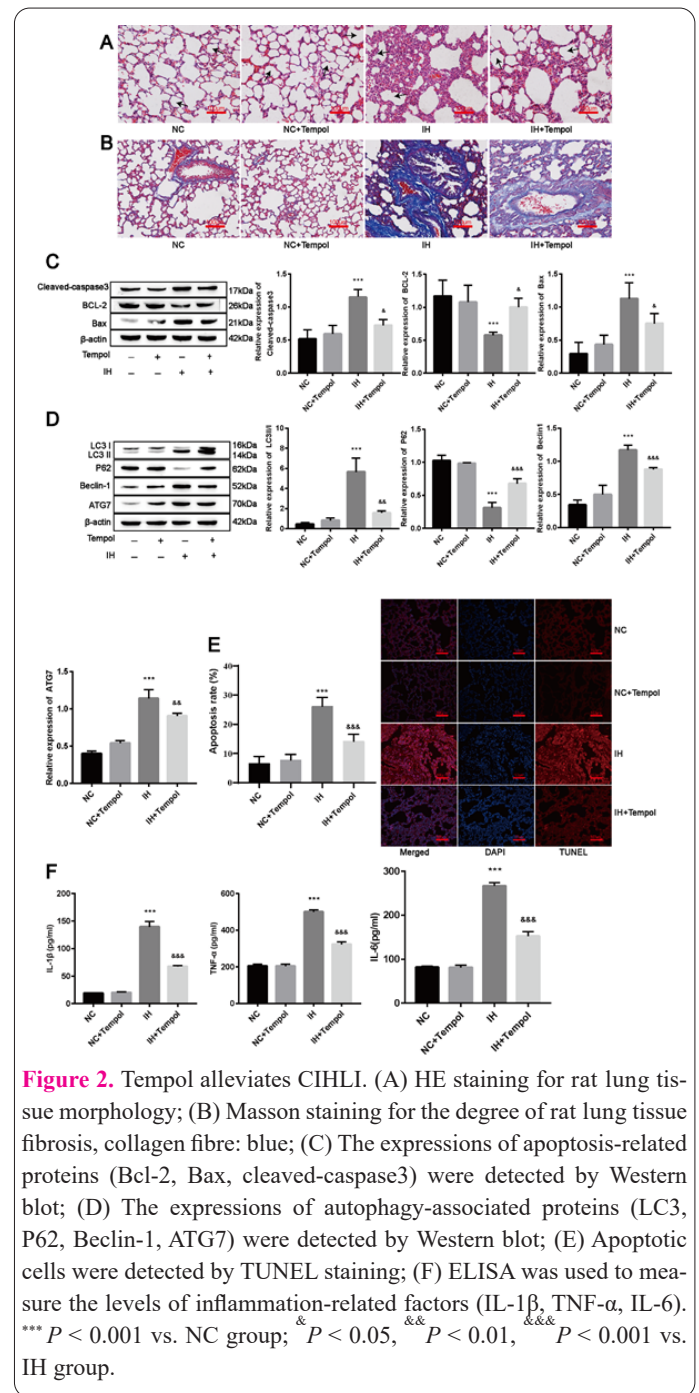


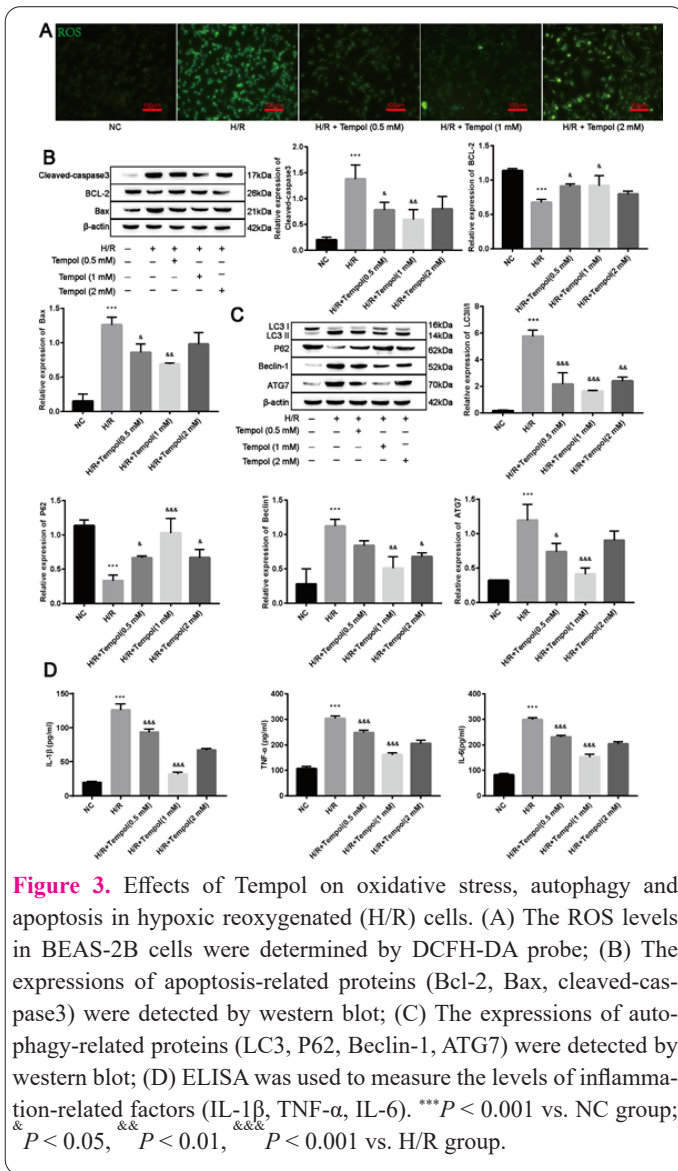
the experimental data showed that the alveolar structure of the NC group and the NC+ Tempol group was normal, with almost no collagen deposition and fibrosis. However, there was a large amount of collagen deposition (blue) and the pulmonary fibrosis in the IH group was more severe, which was significantly improved after adding Tempol (Figure 2B). Moreover, upon observing the western blot results, cleaved-caspase3 and Bax expression showed a high trend, but Bcl-2 presented a low level in the IH group, and treatment with Tempol reversed the expression of apoptosis-related proteins (Figure 2C). We also observed that the ratio of LC3 II/LC3 I and the expressions of Beclin-1 and ATG7 showed an upward trend, but P62 presented a lower level in the IH group. Similarly, the expressions of these autophagy-related proteins were reversed after Tempol treatment (Figure 2D). By analyzing the resulting data from TUNEL staining, we found that the apoptosis rate of cells in rat lung injury tissues decreased significantly after Tempol intervention (Figure 2E). Furthermore, the experimental results obtained from ELISA showed that the levels of inflammatory factors, including TNF- $\alpha$ , IL-6 and IL-1 $\beta$ , in rats with injury decreased significantly after Tempol intervention (Figure 2F). Thus, Tempol has a palliative effect on CIHLI.

### Effects of Tempol on oxidative stress, autophagy and apoptosis in hypoxic reoxygenated (H/R) cells

The human lung epithelial cell line BEAS-2B was treated with Tempol at different concentrations (0.5 mM, 1 mM, 2 mM). A DCFH-DA fluorescence probe was used to measure ROS levels. The results showed that compared with the NC group, the ROS level in the H/R group was significantly increased. Tempol treatment at 0.5 mM and 1 mM effectively reduced ROS levels, but the inhibitory effect of 2 mM Tempol treatment was not obvious (Figure 3A). Western blot detection of apoptosis-related proteins showed that compared with that in the NC group, the expression of cleaved-caspase3 and Bax in the H/R group was upregulated, while the expression of Bcl-2 was downregulated. Tempol treatment at 0.5 mM and 1 mM inhibited the expression of cleaved-caspase3 and Bax and

promoted the expression of Bcl-2. Similarly, 2 mM Tempol had no significant effect on protein expression (Figure 3B). Autophagy-related proteins were detected by Western blotting, and compared with the NC group, the expressions of LC3 II/LC3I, Beclin-1 and ATG7 were upregulated, and the expression of P62 was downregulated in the H/R group. Similarly, Tempol treatment effectively reversed the expression of these proteins (Figure 3C). The expression of inflammatory factors was detected by ELISA. The results showed that compared with the NC group, the expression levels of TNF- $\alpha$ , IL-6 and IL-1 $\beta$  were significantly upregulated in the H/R group. Tempol treatment at 0.5 mM and 1 mM effectively inhibited the expression of inflammatory factors, while Tempol treatment at 2 mM had no significant effect on the expression of inflammatory factors (Figure 3D). The above results showed that Tempol affected the occurrence of H/R-induced autophagy and apoptosis in BEAS-2B cells in a dose-dependent manner, and the effect of 1 mM





Tempol was the most significant. Subsequent experiments were carried out at this concentration.

### Screening miR-145-5p at the animal level

The expression levels of miRNAs in lung tissues of rats in different groups were detected by RT-qPCR. The expression levels of miR-15b-5p and miR-92b-3p showed a clear downward trend, while the expressions of miR-145-5p and miR-18a-5p were significantly increased. Compared with the IH group, after treatment with Tempol, the expressions of miR-15b-5p and miR-92b-3p did not change significantly, the expressions of miR-145-5p and miR-18a-5p were downregulated, and the degree of downregulation of miR-145-5p was greater than that of miR-18a-5p (Figure 4). Therefore, we selected miR-145-5p for the following experiment.

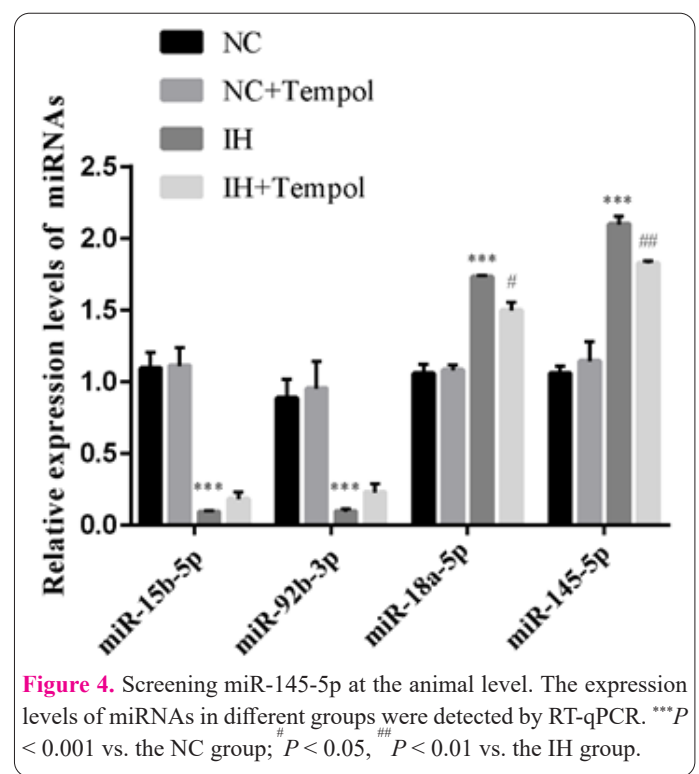
### Effect of miR-145-5p on oxidative stress, autophagy and apoptosis of hypoxic reoxygenated cells

After determining that Tempol treatment can inhibit miR-145-5p expression, we transfected the miR-145-5p mimic and miR-145-5p inhibitor into BEAS-2B cells to observe the effect of miR-145-5p on BEAS-2B autophagy and apoptosis. DCFH-DA fluorescence probe detection of ROS levels showed that transfection with the miR-145-5p inhibitor resulted in a significant decrease in intracellu-

lar ROS content, while the miR-145-5p mimic increased the intracellular ROS content (Figure 5A). The detection of apoptosis-related proteins and autophagy-related proteins by western blot showed that the transfection of the miR-145-5p inhibitor effectively inhibited the expression of apoptotic proteins cleaved-caspase3 and Bax and promoted the expression of anti-apoptotic protein Bcl-2 (Figure 5B). Meanwhile, the expressions of the autophagy-related proteins LC3II/LC3I, Beclin-1 and ATG7 were inhibited, and the expression of the P62 protein was promoted after transfection of the miR-145-5p mimic on apoptosis-associated and autophagy-associated proteins was opposite to that of the miR-145-5p inhibitor. Furthermore, the experimental results obtained from ELISA showed that the levels of inflammatory factors, including TNF- $\alpha$ , IL-6 and IL-1 $\beta$ , decreased significantly in the miR-145-5p inhibitor group but presented the opposite result in the miR-145-5p mimic group (Figure 5D). These results suggest that inhibition of miR-145-5p can effectively inhibit the occurrence of autophagy and apoptosis in human lung epithelial cells under HR conditions.

### Verification of the targeting relationship between miR-145-5p and Nrf2

According to StarBase ([http://www.targetscan.org/vert\\_72/](http://www.targetscan.org/vert_72/)), we found a target binding sequence between Nrf2 and miR-145-5p (Figure 6A). By analyzing the data detected by dual luciferase gene reporter assay, we found that transfection of the miR-145-5p mimic could effectively reduce the fluorescence activity of the Nrf2-WT group but did not affect the fluorescence activity of the Nrf2-MUT group (Figure 6B). The expression of Nrf2 was detected by RT-qPCR, and the results showed that the miR-145-5p mimic could significantly inhibit the expression of Nrf2 (Figure 6C). The above results indicated that miR-145-5p could target and negatively regulate the expression of Nrf2.



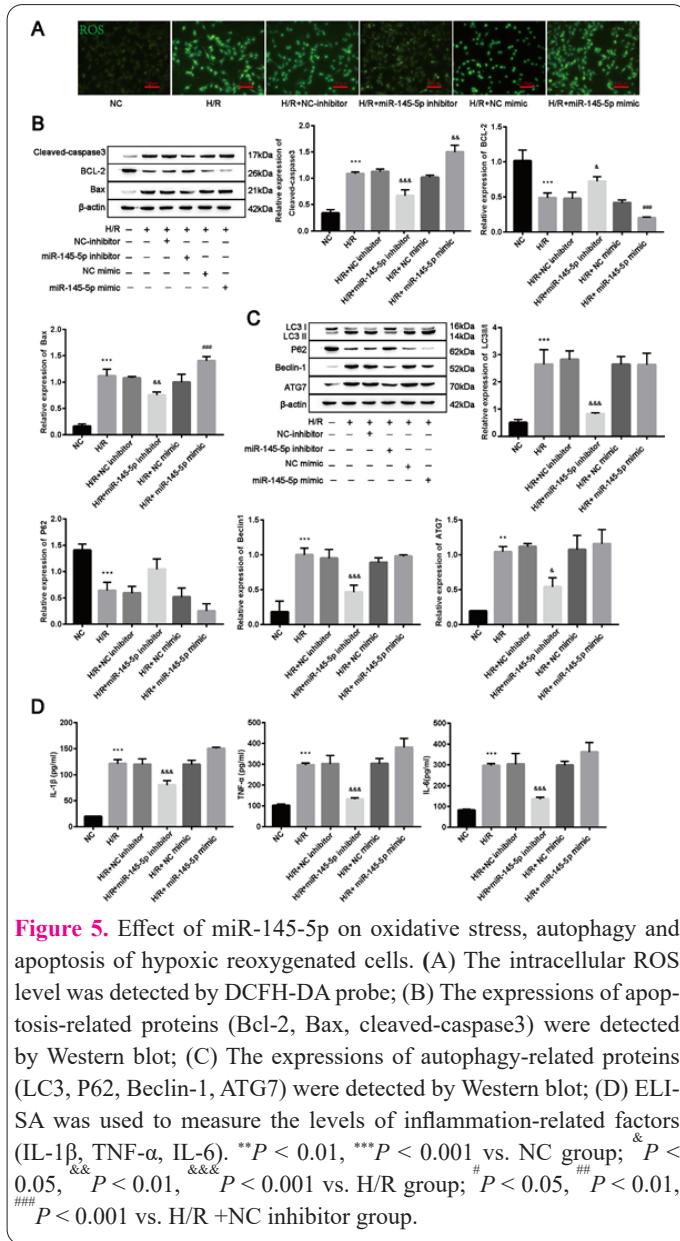


**Figure 5.** Effect of miR-145-5p on oxidative stress, autophagy and apoptosis of hypoxic reoxygenated cells. (A) The intracellular ROS level was detected by DCFH-DA probe; (B) The expressions of apoptosis-related proteins (Bcl-2, Bax, cleaved-caspase3) were detected by Western blot; (C) The expressions of autophagy-related proteins (LC3, P62, Beclin-1, ATG7) were detected by Western blot; (D) ELISA was used to measure the levels of inflammation-related factors (IL-1 $\beta$ , TNF- $\alpha$ , IL-6). \*\* $P < 0.01$ , \*\*\* $P < 0.001$  vs. NC group; &  $P < 0.05$ , &&  $P < 0.01$ , &&&  $P < 0.001$  vs. H/R group; #  $P < 0.05$ , #&  $P < 0.01$ , #&&  $P < 0.001$  vs. H/R +NC inhibitor group.

### Effect of Tempol on oxidative stress, autophagy and apoptosis through the miR-145-5p/Nrf2 signaling pathway

ROS levels were detected by the DCFH-DA fluorescence probe, and the miR-145-5p mimic reversed the effect of Tempol on intracellular ROS content, while intracellular ROS content decreased significantly after overexpression of Nrf2 (Figure 7A). Western blot analysis showed that the miR-145-5p mimic could reverse the inhibitory effects of Tempol on the expression of cleaved-caspase3 and Bax and promote the expression of Bcl-2. Overexpression of Nrf2 weakened the effect of the miR-145-5p mimic on Tempol (Figure 7B). We also found that the ratio of LC3-II/LC3-I, Beclin-1 and ATG7 expression showed an upward trend, and P62 presented a lower level after miR-145-5p mimic transfection. The above proteins showed opposite trends after overexpression of Nrf2 (Figure 7C). ELISA results showed that the miR-145-5p mimic could reverse the inhibitory effect of Tempol on TNF- $\alpha$ , IL-6, and IL-1 $\beta$  expressions after transfection, and overexpression of Nrf2 could effectively weaken the effect of the miR-145-5p mimic on Tempol (Figure 7D). The above results indicate that Tempol inhibits oxidative stress, autophagy, and apoptosis induced by hypoxic reoxygenation

by regulating the miR-145-5p/Nrf2 signaling pathway.

### Tempol attenuates CIHLI through the miR-145-5p/Nrf2 signaling pathway

The tissue morphology was observed through Masson and HE staining. Tempol improved IH-induced lung injury, and an obvious increase in the degree of lung injury treated with the miR-145-5p mimic was observed. The degree of alveolar lysis and inflammatory cell infiltration in lung tissue increased, collagen deposition (blue) increased and pulmonary fibrosis was obvious. However, OE-Nrf2 reversed this effect (Figure 8A-B). Moreover, after observing the western blot results, we found that treatment with the miR-145-5p mimic effectively reversed the inhibitory effects of Tempol on the expression of cleaved-caspase3 and Bax and the promoting effects of Bcl-2. Overexpression of Nrf2 weakened the effect of the miR-145-5p mimic on Tempol (Figure 8C). Compared with the IH group, the expressions of LC3 II/LC3I, Beclin-1 and ATG7 were downregulated, and the expression of P62 was upregulated in the IH+ Tempol group. The expression of autophagy-related proteins was reversed after miR-145-5p mimic treatment, and overexpression of Nrf2 weakened the effects of miR-145-5p (Figure 8D). TUNEL staining was used to detect cell apoptosis in the lung injury tissues of rats. The results showed that the inhibitory effects of Tempol treatment on cell apoptosis were reversed to a certain extent after injection of the miR-145-5p mimic, while OE-Nrf2 significantly reversed the effects of the miR-145-5p mimic (Figure 8E). Serum inflammatory cytokines were detected by ELISA. The results showed that the expression levels of TNF- $\alpha$ , IL-6, and IL-1 $\beta$  in the IH+ Tempol group were downregulated compared with those in the IH group. At the same time, compared with the IH+NC mimic+ Tempol group, the expression levels of inflammatory factors were increased in the IH+miR-145-5p mimic+ Tempol group, while OE-Nrf2 effectively reduced

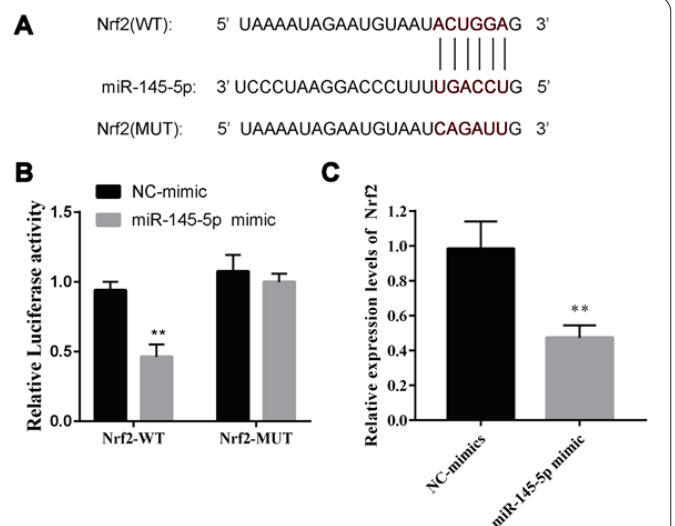


**Figure 6.** Verification of the targeting relationship between miR-145-5p and Nrf2. (A) StarBase ([http://www.targetscan.org/vert\\_72/](http://www.targetscan.org/vert_72/)) was used to predict the binding sites between miR-145-5p and Nrf2; (B) Luciferase reporter gene assay confirmed the binding relationship between Nrf2 and miR-145-5p; (C) The mRNA expression level of Nrf2 was detected by RT-qPCR. \*\*  $P < 0.01$  vs. NC group.

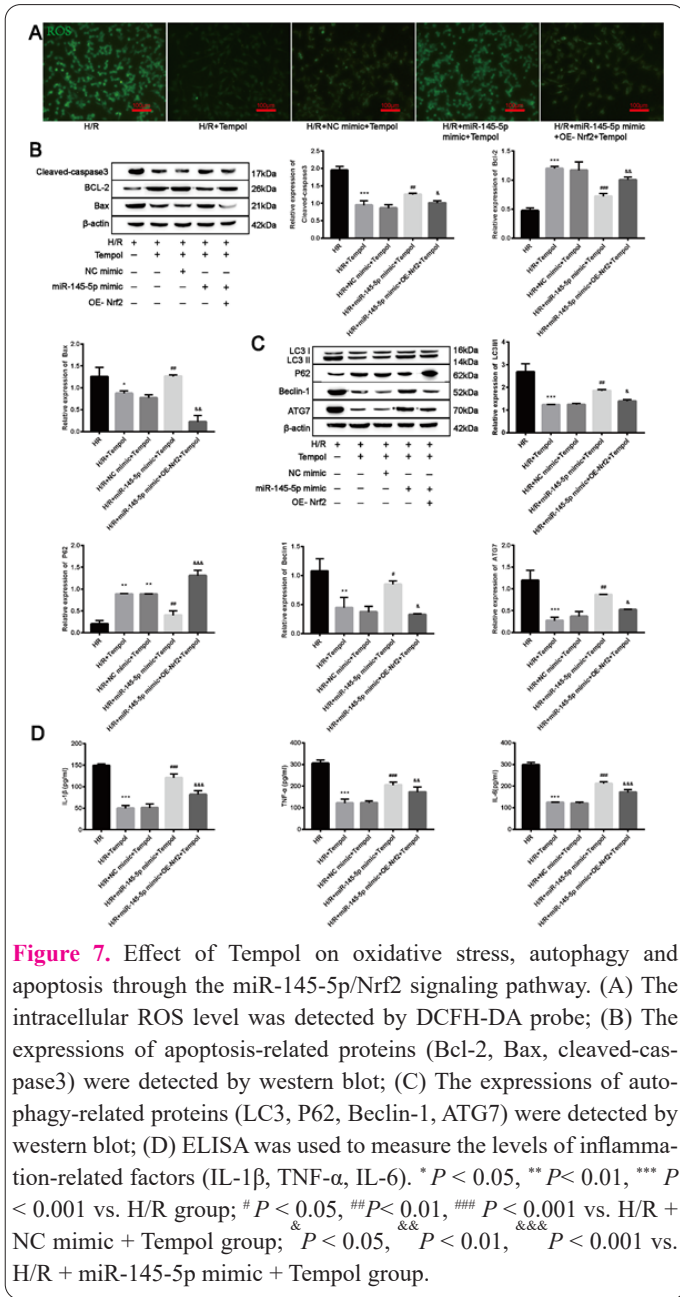


**Figure 7.** Effect of Tempol on oxidative stress, autophagy and apoptosis through the miR-145-5p/Nrf2 signaling pathway. (A) The intracellular ROS level was detected by DCFH-DA probe; (B) The expressions of apoptosis-related proteins (Bcl-2, Bax, cleaved-caspase3) were detected by western blot; (C) The expressions of autophagy-related proteins (LC3, P62, Beclin-1, ATG7) were detected by western blot; (D) ELISA was used to measure the levels of inflammation-related factors (IL-1 $\beta$ , TNF- $\alpha$ , IL-6). \*  $P < 0.05$ , \*\*  $P < 0.01$ , \*\*\*  $P < 0.001$  vs. H/R group; #  $P < 0.05$ , ##  $P < 0.01$ , ###  $P < 0.001$  vs. H/R + NC mimic + Tempol group; &  $P < 0.05$ , &&  $P < 0.01$ , &&&  $P < 0.001$  vs. H/R + miR-145-5p mimic + Tempol group.

the expression levels of inflammatory factors (Figure 8F). These results demonstrated that Tempol alleviated CIHLI by activating the miR-145-5p/Nrf2 signaling pathway.

### Discussion

There are many people with OSA in the world, and morbidity is rising and mostly occurs in middle-aged and elderly men (19). OSA is a complex somatic disease that has a significant impact on quality of life, mortality rate, and long-term cardiovascular outcomes (20). Because the disease has a very large group, it also has resulted in certain pressure for social development. At present, researchers are not clear regarding the pathogenic mechanism of OSAHS, but it is clear that patients will have repeated upper airway obstruction and intermittent hypoxia-reoxygenation during sleep, thereby changing the level of their own oxidative stress. Chronic intermittent hypoxia aggravates skeletal muscle aging by downregulating the expression of Klc1/grx1 through the Wnt/ $\beta$ -catenin pathway (21). Zhang Huina et al. (22) showed that extracellular vesicle-derived miR-144 acted as a new mechanism for chronic

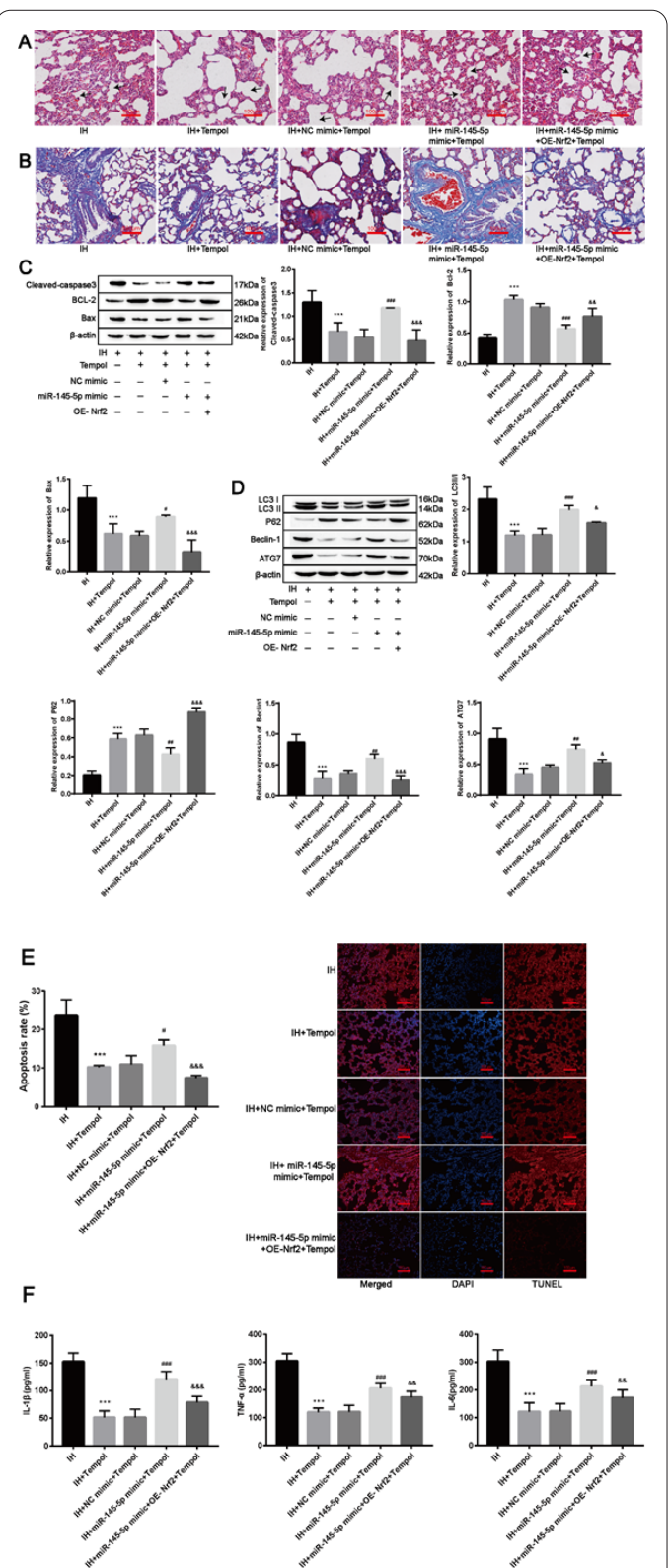


**Figure 8.** Tempol attenuates CIHLI through the miR-145-5p/Nrf2 signaling pathway. (A) HE staining for the rat lung tissue morphology; (B) Masson staining was used to observe pulmonary fibrosis in rats, collagen fibre: blue; (C) The expressions of apoptosis-related proteins (Bcl-2, Bax, cleaved-caspase3) were detected by western blot; (D) The expressions of autophagy-related proteins (LC3, P62, Beclin-1, ATG7) were detected by western blot; (E) Apoptotic cells were detected by TUNEL staining; (F) ELISA was used to measure the levels of inflammation-related factors (IL-1 $\beta$ , TNF- $\alpha$ , IL-6). \*\*\*  $P < 0.001$  vs. IH group; #  $P < 0.05$ , ###  $P < 0.001$  vs. IH+ NC mimic + Tempol group; &  $P < 0.05$ , &&  $P < 0.01$ , &&&  $P < 0.001$  vs. IH + miR-145-5p mimic + Tempol group.

intermittent hypoxia-induced endothelial dysfunction. It has been reported that the oxidative stress and inflammatory response induced by IH exposure play an important role in the pathogenesis of tumor metastasis, and the use of antioxidants, such as Tempol, may provide a new vision and further research direction for the treatment of OSA-related cancer (23). We found that Tempol improved lung function by inhibiting CIHLI in Wistar rats, reduced oxidative stress and inflammatory cytokine release in BEAS-2B cells, and inhibited ROS-mediated autophagy and apoptosis. Mechanistically, Tempol plays a role in alleviating lung injury induced by chronic intermittent hypoxia by regulating the miR-145-5p/Nrf2 signaling pathway.

Nrf2 plays a key role as a transcription factor in oxidative stress, and Tempol can alleviate the oxidative stress of lung tissue induced by IH by activating the Nrf2/HO-1 signaling pathway (24). After reviewing the literature, we found that the Nrf2/ARE pathway ameliorates intermittent hypoxia-induced damage in pancreatic cells (25). Moreover, it has been reported that triptolide plays a role in the treatment of pancreatitis (AP) by activating the expression of Nrf2 (26). In OSA cells and animal models, overexpression of Nrf2 could effectively inhibit H/R-induced apoptosis and oxidative stress, as well as IH-induced lung injury in rats.

There is growing evidence that oxidative stress and inflammation pervade lung injury and are inextricably linked to disease course and mortality (27-29). Tempol is a small molecule free radical scavenger that can penetrate cell membranes and has the function of preventing and treating lung damage (24). Moreover, studies have shown that Tempol has multiple active functions, including antioxidant, anti-inflammatory, anti-lipid metabolism, cardiovascular and neuroprotective activities (30-32). Tempol reduces inflammation and oxidative damage in mice modeled by cigarette smoke by activating the Nrf2 pathway as well as reducing neutrophil infiltration (12). Additionally, administration of Tempol to cells attenuates warm ischemic injury to lung function in heartless donors (33). Furthermore, the antioxidant activity of Tempol is involved in ameliorating oxidative DNA damage in Fanconi anemia fibroblasts and mice, thereby delaying tumor development (34). Consistent with other studies, we also found positive effects of tempol as an antioxidant. In our study, we found that Tempol can effectively ameliorate IH-induced lung injury in rats and inhibit H/R-induced oxidative stress in BEAS-2B cells, that is, effectively reducing the level of ROS in cells. In addition, Tempol inhibited the expressions of the proapoptotic proteins cleaved-caspase3 and Bax and promoted the expression of the antiapoptotic protein Bcl-2. The expressions of TNF- $\alpha$ , IL-6 and IL-1 $\beta$  were also inhibited.

To further investigate the mechanism of chronic intermittent lung injury, we found that miR-145-5p was significantly reduced at the animal level after Tempol treatment. ROS-mediated autophagy and apoptosis of cells are known to simultaneously promote cellular oxidative stress and inflammatory responses (35-37). According to the literature, the overexpression of miR-145-5p can improve the early decline in lung function in children with asthma, and the decreased expression of miR-145-5p can promote the early decline in long-term lung function (38). Meanwhile, miR-145-5p activates the PRKCI/Akt/mTOR signaling pathway to inhibit autophagy and promote can-

cer progression and chemotherapy resistance in laryngeal squamous cell carcinoma (39). MiR-145-5p regulates thymic epithelial tumor genetic expression (40). As most previous studies reported, we also found that miR-145-5p plays a negative role in I/H-induced lung injury. Our study showed that transfection of the miR-145-5p inhibitor in BEAS-2B cells could effectively inhibit H/R-induced oxidative stress, autophagy and apoptosis, while transfection of the miR-145-5p mimic showed the opposite results. In addition, the miR-145-5p mimic effectively reversed the inhibitory effects of Tempol on cellular oxidative stress and lung injury in rats. We also found that miR-145-5p targeting negatively regulated the expression of Nrf2, and overexpression of Nrf2 can reverse the effects of the miR-145-5p mimic to a certain extent. This suggests that Tempol can improve lung injury caused by chronic IH by regulating the miR-145-5p/Nrf2 molecular axis.

This study found that Tempol could inhibit inflammatory response and oxidative stress, and effectively improve IH-induced lung injury. In addition, we elucidated the mechanism that Tempol alleviated lung injury by regulating the occurrence of oxidative stress mediated by the miR-145-5p/Nrf2 axis. This provides new ideas and potential therapeutic targets for the treatment of OSA-associated lung injury.

#### Funding

This study was supported by the National Natural Science Foundation of China [81960025].

#### Availability of data and materials

The datasets used and/or analyzed during the current study are available from the corresponding author upon reasonable request.

#### Authors' contributions

Conceptualization, Li Ai and Ran Li; methodology, Li Ai, Yongxia Li and Xiaona Wang; software, Zhijuan Liu; validation, Bing Hai; formal analysis, Ran Li, Zhijuan Liu and Xiaona Wang; investigation, Li Ai and Yongxia Li; resources, Li Ai and Yongxia Li; data curation, Ran Li and Bing Hai; writing—original draft preparation, Li Ai and Yongxia Li; writing—review and editing, Li Ai and Yongxia Li; visualization, Ran Li, Zhijuan Liu and Xiaona Wang; supervision, Li Ai and Yongxia Li; funding acquisition, Li Ai and Yongxia Li. All authors have read and agreed to the published version of the manuscript.

#### Ethics approval and consent to participate

All authors confirm that all the methods/studies were in accordance with the ARRIVE guidelines. All animal experiments were approved by the Experimental Animal Ethics Committee of Kunming Medical University(kmmu20211432).

#### Competing interests

The authors declare that they have no competing interests.

#### References

1. Labarca G, Gower J, Lamperti L, et al. Chronic intermittent hypoxia in obstructive sleep apnea: a narrative review from pathophysiological pathways to a precision clinical approach. *Sleep Breath.* 2020;24(2):751-760.

2. Wu G, Lee YY, Gulla EM, et al. Short-term exposure to intermittent hypoxia leads to changes in gene expression seen in chronic pulmonary disease. *Elife*. 2021;10.
3. Zhang P, Wang Y, Wang H, et al. Sesamol alleviates chronic intermittent hypoxia-induced cognitive deficits via inhibiting oxidative stress and inflammation in rats. *Neuroreport*. 2021;32(2):105-111.
4. Hou Y, Xu N, Li S, et al. Mechanism of SMND-309 against lung injury induced by chronic intermittent hypoxia. *Int Immunopharmacol*. 2022;105:108576.
5. Jia L, Hao H, Wang C, et al. Etomidate attenuates hyperoxia-induced acute lung injury in mice by modulating the Nrf2/HO-1 signaling pathway. *Exp Ther Med*. 2021;22(1):785.
6. Bellezza I, Giambanco I, Minelli A, et al. Nrf2-Keap1 signaling in oxidative and reductive stress. *Biochim Biophys Acta Mol Cell Res*. 2018;1865(5):721-733.
7. Saha S, Buttari B, Panieri E, et al. An Overview of Nrf2 Signaling Pathway and Its Role in Inflammation. *Molecules*. 2020;25(22).
8. Yan J, Li J, Zhang L, et al. Nrf2 protects against acute lung injury and inflammation by modulating TLR4 and Akt signaling. *Free Radic Biol Med*. 2018;121:78-85.
9. Xu W, Wang M, Cui G, et al. Astaxanthin Protects OTA-Induced Lung Injury in Mice through the Nrf2/NF-kappaB Pathway. *Toxins (Basel)*. 2019;11(9).
10. Ewees MG, Messiha BAS, Abdel-Bakky MS, et al. Tempol, a superoxide dismutase mimetic agent, reduces cisplatin-induced nephrotoxicity in rats. *Drug Chem Toxicol*. 2019;42(6):657-664.
11. Park WH. Tempol differently affects cellular redox changes and antioxidant enzymes in various lung-related cells. *Sci Rep*. 2021;11(1):14869.
12. Silva DAD, Correia TML, Pereira R, et al. Tempol reduces inflammation and oxidative damage in cigarette smoke-exposed mice by decreasing neutrophil infiltration and activating the Nrf2 pathway. *Chem Biol Interact*. 2020;329:109210.
13. Tang M, Zhang L, Zhu Z, et al. Overexpression of miR-506-3p Aggravates DBP-Induced Testicular Oxidative Stress in Rats by Downregulating ANXA5 via Nrf2/HO-1 Signaling Pathway. *Oxid Med Cell Longev*. 2020;2020:4640605.
14. Pelullo M, Savi D, Quattrucci S, et al. miR-125b/NRF2/HO-1 axis is involved in protection against oxidative stress of cystic fibrosis: A pilot study. *Exp Ther Med*. 2021;21(6):585.
15. Huang Y, Huang L, Zhu G, et al. Downregulated microRNA-27b attenuates lipopolysaccharide-induced acute lung injury via activation of NF-E2-related factor 2 and inhibition of nuclear factor kappaB signaling pathway. *J Cell Physiol*. 2019;234(5):6023-6032.
16. Qiao L, Li RX, Hu SG, et al. microRNA-145-5p attenuates acute lung injury via targeting ETS2. *Kaohsiung J Med Sci*. 2022;38(6):565-573.
17. Yu YL, Yu G, Ding ZY, et al. Overexpression of miR-145-5p alleviated LPS-induced acute lung injury. *J Biol Regul Homeost Agents*. 2019;33(4):1063-1072.
18. Li Y, Gao M, Yin LH, et al. Dioscin ameliorates methotrexate-induced liver and kidney damages via adjusting miRNA-145-5p-mediated oxidative stress. *Free Radic Biol Med*. 2021;169:99-109.
19. Gu H, Ru Y, Wang W, et al. Orexin-A Reverse Bone Mass Loss Induced by Chronic Intermittent Hypoxia Through OX1R-Nrf2/HIF-1alpha Pathway. *Drug Des Devel Ther*. 2022;16:2145-2160.
20. Brodie KD, Goldberg AN. Obstructive Sleep Apnea: A Surgeon's Perspective. *Med Clin North Am*. 2021;105(5):885-900.
21. Guo H, Zhang Y, Han T, et al. Chronic intermittent hypoxia aggravates skeletal muscle aging by down-regulating Klf1/grx1 expression via Wnt/beta-catenin pathway. *Arch Gerontol Geriatr*. 2021;96:104460.
22. Zhang H, Peng L, Wang Y, et al. Extracellular vesicle-derived miR-144 as a novel mechanism for chronic intermittent hypoxia-induced endothelial dysfunction. *Theranostics*. 2022;12(9):4237-4249.
23. Li L, Ren F, Qi C, et al. Intermittent hypoxia promotes melanoma lung metastasis via oxidative stress and inflammation responses in a mouse model of obstructive sleep apnea. *Respir Res*. 2018;19(1):28.
24. Wang Y, Hai B, Ai L, et al. Tempol relieves lung injury in a rat model of chronic intermittent hypoxia via suppression of inflammation and oxidative stress. *Iran J Basic Med Sci*. 2018;21(12):1238-1244.
25. Li CG, Ni CL, Yang M, et al. Honokiol protects pancreatic beta cell against high glucose and intermittent hypoxia-induced injury by activating Nrf2/ARE pathway in vitro and in vivo. *Biomed Pharmacother*. 2018;97:1229-1237.
26. Yang J, Tang X, Ke X, et al. Triptolide Suppresses NF-kappaB-Mediated Inflammatory Responses and Activates Expression of Nrf2-Mediated Antioxidant Genes to Alleviate Caerulein-Induced Acute Pancreatitis. *Int J Mol Sci*. 2022;23(3).
27. Guo Y, Liu Y, Zhao S, et al. Oxidative stress-induced FABP5 S-glutathionylation protects against acute lung injury by suppressing inflammation in macrophages. *Nat Commun*. 2021;12(1):7094.
28. Yang H, Lv H, Li H, et al. Oridonin protects LPS-induced acute lung injury by modulating Nrf2-mediated oxidative stress and Nrf2-independent NLRP3 and NF-kappaB pathways. *Cell Commun Signal*. 2019;17(1):62.
29. Li T, Wu YN, Wang H, et al. Dapk1 improves inflammation, oxidative stress and autophagy in LPS-induced acute lung injury via p38MAPK/NF-kappaB signaling pathway. *Mol Immunol*. 2020;120:13-22.
30. Li L, Lai EY, Luo Z, et al. Superoxide and hydrogen peroxide counterregulate myogenic contractions in renal afferent arterioles from a mouse model of chronic kidney disease. *Kidney Int*. 2017;92(3):625-633.
31. Neil S, Huh J, Baronas V, et al. Oral administration of the nitroxide radical TEMPOL exhibits immunomodulatory and therapeutic properties in multiple sclerosis models. *Brain Behav Immun*. 2017;62:332-343.
32. Salvi A, Patki G, Khan E, et al. Protective Effect of Tempol on Buthionine Sulfoximine-Induced Mitochondrial Impairment in Hippocampal Derived HT22 Cells. *Oxid Med Cell Longev*. 2016;2016:5059043.
33. Hodyc D, Hnilickova O, Hampl V, et al. Pre-arrest administration of the cell-permeable free radical scavenger tempol reduces warm ischemic damage of lung function in non-heart-beating donors. *J Heart Lung Transplant*. 2008;27(8):890-897.
34. Zhang QS, Eaton L, Snyder ER, et al. Tempol protects against oxidative damage and delays epithelial tumor onset in Fanconi anemia mice. *Cancer Res*. 2008;68(5):1601-1608.
35. Li F, Li J, Wang PH, et al. SARS-CoV-2 spike promotes inflammation and apoptosis through autophagy by ROS-suppressed PI3K/AKT/mTOR signaling. *Biochim Biophys Acta Mol Basis Dis*. 2021;1867(12):166260.
36. Racanelli AC, Kikkers SA, Choi AMK, et al. Autophagy and inflammation in chronic respiratory disease. *Autophagy*. 2018;14(2):221-232.
37. Liu M, Sun T, Li N, et al. BRG1 attenuates colonic inflammation and tumorigenesis through autophagy-dependent oxidative stress sequestration. *Nat Commun*. 2019;10(1):4614.
38. Tiwari A, Li J, Kho AT, et al. COPD-associated miR-145-5p is downregulated in early-decline FEV(1) trajectories in childhood asthma. *J Allergy Clin Immunol*. 2021;147(6):2181-2190.

39. Gao W, Guo H, Niu M, et al. circPARD3 drives malignant progression and chemoresistance of laryngeal squamous cell carcinoma by inhibiting autophagy through the PRKCI-Akt-mTOR pathway. *Mol Cancer*. 2020;19(1):166.
40. Bellissimo T, Ganci F, Gallo E, et al. Thymic Epithelial Tumors phenotype relies on miR-145-5p epigenetic regulation. *Mol Cancer*. 2017;16(1):88.